Chromosome misalignment is associated with PLK1 activity at cenexin-positive mitotic centrosomes

Erica G. Colicino[a,b,†], Katrina Stevens[c], Erin Curtis[a], Lindsay Rathbun[a], Michael Bates[a], Julie Manikas[a], Jeffrey Amack[b], Judy Freshour[a], and Heidi Hehnly[a,*]
[a]Biology Department, Syracuse University, Syracuse, NY 13210; [b]Department of Cell and Developmental Biology, Upstate Medical University, Syracuse, NY 13210; [c]Biology Department, Clarkson University, Potsdam, NY 13699

ABSTRACT **The mitotic kinase, polo-like kinase 1 (PLK1), facilitates the assembly of the two mitotic spindle poles, which are required for the formation of the microtubule-based spindle that ensures appropriate chromosome distribution into the two forming daughter cells. Spindle poles are asymmetric in composition. One spindle pole contains the oldest mitotic centriole, the mother centriole, where the majority of cenexin, the mother centriole appendage protein and PLK1 binding partner, resides. We hypothesized that PLK1 activity is greater at the cenexin-positive older spindle pole. Our studies found that PLK1 asymmetrically localizes between spindle poles under conditions of chromosome misalignment, and chromosomes tend to misalign toward the oldest spindle pole in a cenexin- and PLK1-dependent manner. During chromosome misalignment, PLK1 activity is increased specifically at the oldest spindle pole, and this increase in activity is lost in cenexin-depleted cells. We propose a model where PLK1 activity elevates in response to misaligned chromosomes at the oldest spindle pole during metaphase.**

Monitoring Editor
Yukiko Yamashita
University of Michigan

Received: Dec 26, 2018
Revised: Mar 28, 2019
Accepted: Apr 25, 2019

INTRODUCTION

Mitotic cell division is a process whereby genetic material is duplicated, separated, and packaged to yield two daughter cells. This process relies heavily on the spatial and temporal synchronization of signaling activity at the mitotic spindle, a structure that segregates the chromosomes and guides them toward the daughter cells. The mitotic kinase, polo-like kinase 1 (PLK1), is a major regulator of this process that works to ensure bipolar spindle formation and chromosome alignment at the metaphase plate. This is accomplished by PLK1-scaffold interactions at the mitotic centrosomes/spindle poles, which modulate the recruitment of centrosome components SAS-4, γ-tubulin, γ-TuRC, pericentrin, and CEP215 (reviewed in Colicino and Hehnly, 2018). Their recruitment is initiated after PLK1-dependent SAS-4 phosphorylation (Ramani *et al.*, 2018). This phosphorylation allows SAS-4 expansion to occur, followed by the recruitment of CEP215 and γ-tubulin and subsequent expansion of the pericentriolar material (PCM), playing a crucial role in mitotic centrosome/spindle pole formation during division (Ramani *et al.*, 2018). However, it is unclear whether PLK1 is additionally regulated between the two spindle poles during cell division.

Owing to the nature of centriole duplication, the two spindle poles are inherently asymmetric from one another. The oldest (mother) spindle pole is enriched with the centriole appendage protein cenexin, compared to the youngest spindle pole (daughter; Vertii *et al.*, 2015; Hung *et al.*, 2016). During interphase, mother centriole appendages assist in centrosome positioning (Hung *et al.*, 2016) and primary cilia formation by anchoring the oldest centriole (known here as the basal body) to the cell membrane to form

This article was published online ahead of print in MBoC in Press (http://www.molbiolcell.org/cgi/doi/10.1091/mbc.E18-12-0817) on May 1, 2019.

E.C. and H.H. designed and E.C., M.B., L.R., K.S., J.M., and H.H. conducted experiments and analyzed the data. J.A. provided zebrafish embryos and husbandry knowledge. J.F. constructed all vectors utilized. E.C. and H.H. wrote the manuscript, contributing to multiple rounds of edits.

†Present address: Department of Cell and Developmental Biology, University of Michigan Medical School, Ann Arbor, MI 48109.

*Address correspondence to: Heidi Hehnly (hhehnly@syr.edu).

Abbreviations used: CENPA, centromere protein A; CEP164, centrosome protein 164; CEP215, centrosome protein 215; CFP, cyan fluorescent protein; DAPI, 4′,6-diamidino-2-phenylindole; DDR, DNA damage repair; FRAP, fluorescence recovery after photobleaching; FRET, fluorescence resonance energy transfer; γ-TuRC, γ-tubulin ring complex; GFP, green fluorescent protein; GSD, ground state depletion; HPF, hours postfertilization; LUT, look-up table; PACT, pericentrin AKAP centrosomal targeting; PCM, pericentriolar material; PLK1, Polo-like kinase 1; ROI, region of Interest; RPE, retinal pigment epithelial; SAS-4, spindle assembly abnormal protein 4; shRNA, short-hairpin RNA; SIM, structured illumination microscopy; YFP, yellow fluorescent protein.

the primary cilia (reviewed in Kobayashi and Dynlacht, 2011, and Vertii *et al.*, 2016). Prior to mitotic onset, PLK1 is recruited to the basal body where it assists in ciliary disassembly (Wang *et al.*, 2013). Cenexin regulates appendage formation and has also been identified as a PLK1 binding partner (Soung *et al.*, 2006, 2009). Previous work utilizing ground state depletion (GSD) identified a modest, but significant, enrichment of PLK1 at the mother (cenexin-positive) spindle pole in fixed in vitro metaphase cells (Hehnly *et al.*, 2015). This study suggests an inherent asymmetry in PLK1 distribution that is dependent on centrosome age. During division, cenexin has been implicated in multiple processes, including modulating preferential chromosome misalignment toward the oldest spindle pole in the event of mitotic error (Gasic *et al.*, 2015). Knowing this, we wanted to test the hypothesis that PLK1 localization and activity is asymmetrically regulated between the two spindle poles through the presence of cenexin at the mother spindle pole, which can modulate directional chromosome misalignment.

Using a multidisciplinary approach, we found a significant asymmetry in PLK1 localization and activity between spindle poles in in vivo zebrafish studies and in vitro tissue culture. From here, we tested whether the propensity for chromosomes to misalign toward one spindle pole altered PLK1 activity. We further examined whether altering PLK1 activity influences the preferential misalignment of lagging chromosomes toward the oldest spindle pole.

RESULTS

Asymmetric distribution of PLK1 in zebrafish and mammalian cells

In mammalian dividing cells, PLK1 is up-regulated during mitosis. During this time, it is enriched at spindle poles and kinetochores, specifically from prometaphase to metaphase (Kishi *et al.*, 2009; Colicino and Hehnly, 2018). Following metaphase exit, PLK1 transitions from kinetochores to the cytokinetic furrow, where it is subsequently concentrated at the forming midbody (Burkard *et al.*, 2007; Kishi *et al.*, 2009; Colicino *et al.*, 2018; modeled in Supplemental Figure 1A). The subcellular distribution of PLK1 in mammalian cells has predominately been studied in in vitro cell culture models. However, in vitro systems do not always represent what is happening in vivo. Here, we examine the temporal and spatial regulation of PLK1 during division first in a developing vertebrate embryo (Figure 1, A–E) and then in in vitro cell culture (Figure 1, F–I). Fertilized embryos were injected with 100 pg of PLK1-mCherry mRNA. Injected embryos were imaged using confocal microscopy 4.5 h postfertilization (hpf). At this time, embryonic cells are proliferating asynchronously (Kimmel *et al.*, 1995), and proliferating cells can be distinguished via PLK1 expression (Supplemental Figure 1, A–D). By magnifying the PLK1-mCherry–positive subpopulation, a distinct subcellular distribution of PLK1-mCherry at spindle poles and kinetochores was noted (Supplemental Figure 1, D and E). The spatial and temporal distribution of PLK1-mCherry in a single dividing cell was monitored over a 360 s time span. PLK1-mCherry transitions from spindle pole and kinetochore localization in metaphase to cytokinetic furrow localization during cytokinesis where it becomes concentrated at the cytokinetic midbody (Figure 1A and Supplemental Video 1).

Upon investigation of the integrated intensity of PLK1-mCherry between spindle poles in metaphase cells within the zebrafish embryo, we noted that one spindle pole has a significantly larger proportion of PLK1-mCherry compared with the other (Figure 1Ba′; Fire look-up table [LUT]). This is clearly demonstrated when the maximum projection of a single metaphase cell (Figure 1Ba′) is presented as a three-dimensional (3D) surface plot (Figure 1Bb′), where each peak represents a spindle pole (labeled with 1 and 2). The spindle pole peak on the left (1) presents with 10% greater PLK1 fluorescence intensity than its partnering spindle pole peak on the right (2; Figure 1Bb′). To validate this finding, we measured PLK1 fluorescence intensity between spindle pole pairs over 49 metaphase cells from 10 embryos. The spindle pole with the highest intensity was binned as pole 1 and the pole with the lowest intensity was binned as pole 2. From this data set, one spindle pole consistently contained 10.31 ± 1.14% less PLK1-mCherry compared with the other (Figure 1C). We then examined whether this asymmetry was present throughout a 150 s time course of a prometaphase cell transitioning through metaphase (Figure 1, D and E). This was measured by placing a region of interest (ROI) over spindle poles 1 and 2. The integrated intensity of PLK1-mCherry within this region was plotted over 150 s with images taken every 30 s. The graph demonstrates that spindle poles present with asymmetric PLK1 distribution as cells exit prometaphase (Figure 1E; beginning at 60 s time point). These findings suggest an inherent asymmetry in the amount of PLK1 between the two spindle poles that is similar to the asymmetry reported under in vitro fixed cell conditions using GSD (Hehnly *et al.*, 2015).

To determine whether this inherent PLK1 asymmetry between metaphase spindle poles is conserved in live mammalian cells, we employed a retinal pigment epithelial (RPE) cell line that stably expresses GFP-PLK1 at endogenous levels (Colicino *et al.*, 2018). Fluorescence recovery after photobleaching (FRAP) was performed. To do this, a ROI was placed over both spindle poles (Figure 1F), where a 488-nm laser was applied. Upon application of the laser, GFP-PLK1 fluorescence within the regions was bleached. After 1.6 s, GFP-PLK1 signal returns to that region (Figure 1F and Supplemental Video 2). A 3D surface plot was performed for the metaphase cell pre-FRAP (–1.2 s), during the FRAP (0 s), and post-FRAP (1.6 s; Figure 1F). At –1.2 s (pre-FRAP), pole 1 contained significantly more GFP-PLK1 than the other (pole 2). At 0 s, GFP-PLK1 at both poles was successfully bleached. At 1.6 s, pole 1 returned to have an elevated amount of GFP-PLK1 compared with spindle pole 2 (Figure 1F), suggesting an increased exchange of GFP-PLK1 at pole 1. Along these same lines, we determined over multiple metaphase cells that spindle pole 2 contained 14.70 ± 4.12% less GFP-PLK1 compared with pole 1 (Figure 1G). These findings are strikingly similar to the differences in GFP-PLK1 between the two spindle poles observed in metaphase cells within the zebrafish embryo, where one pole had 10.31 ± 1.14% less PLK1 than the other (Figure 1C). Together, this suggests a conserved mechanism for an asymmetric distribution of PLK1 between the two spindle poles.

Our findings demonstrate an asymmetry in PLK1 distribution between the two spindle poles; however, a difference in distribution does not necessarily confer a difference in PLK1 activity. To test activity, we utilized a centrosome-localized PLK1 activity fluorescence resonance energy transfer (FRET) biosensor that we developed and controlled for in Colicino *et al.*, 2018. This biosensor can be successfully utilized under either live or fixed conditions (Colicino *et al.*, 2018). The PLK1 activity FRET biosensor is composed of monomeric cyan fluorescent protein (CFP) and yellow fluorescent protein (YFP) flanking a c-jun PLK1 substrate sequence and an FHA2-phosphobinding domain, anchored to centrosomes by the pericentrin-AKAP450 centrosomal-targeting (PACT) domain using a 10 amino acid linker (Figure 1H; Colicino *et al.*, 2018). Active-PLK1 phosphorylates the c-jun region, causing a conformational change in the biosensor and a decrease in FRET between CFP and YFP. We plotted the inverse FRET ratio, such that an increase in this ratio would correspond to an increase in PLK1 activity (Figure 1I; Colicino *et al.*, 2018). Using this biosensor, we measured the inverse FRET ratio in dividing HeLa cells and binned, from a single metaphase

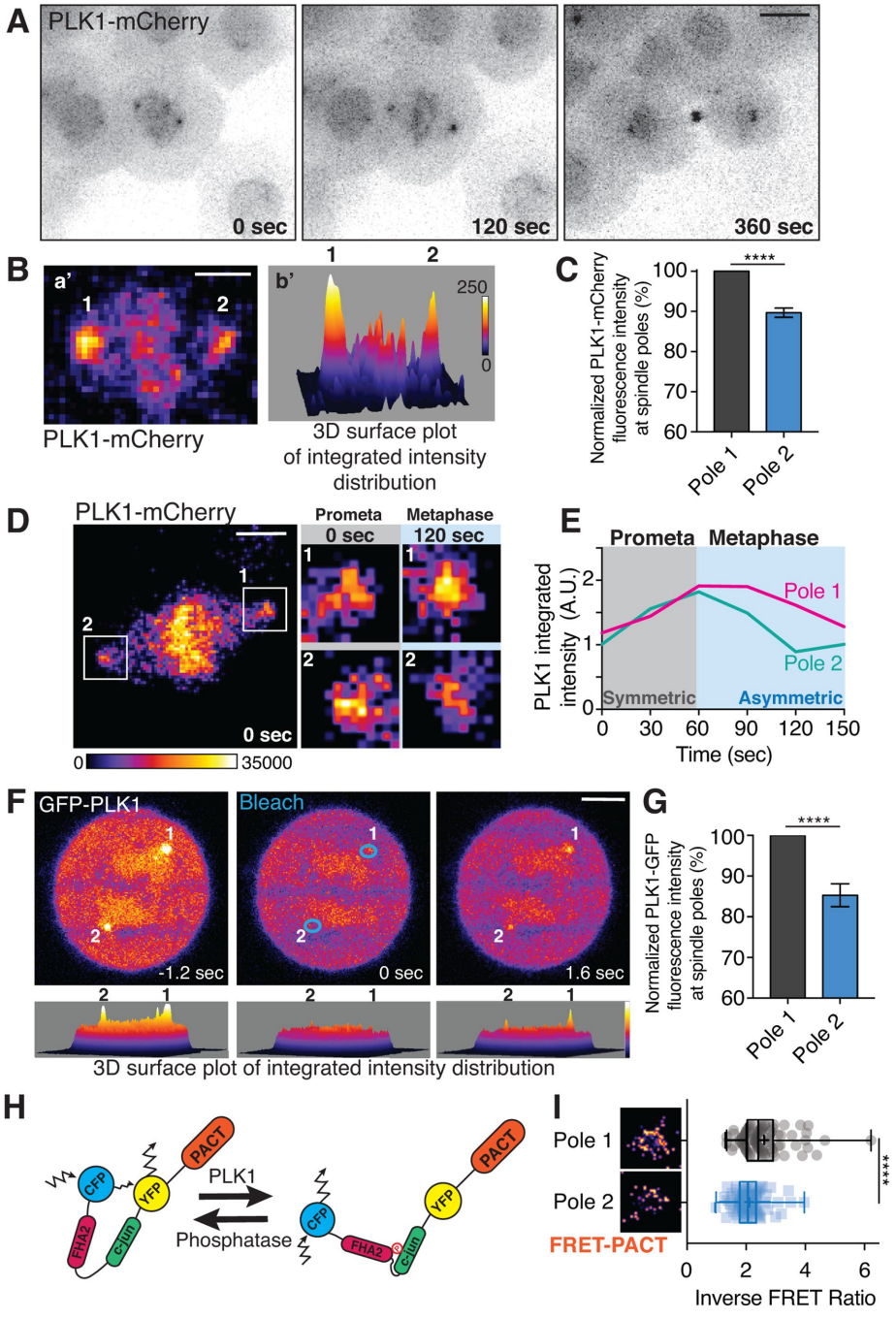

FIGURE 1: PLK1 asymmetric distribution between spindle poles is conserved in vivo (zebrafish) and in vitro (mammalian cell culture). (A–E) Data from a 4.5 hpf embryo expressing PLK1-mCherry. (A) Confocal maximum projections of a single mitotic cell taken from prometaphase through cytokinesis expressing PLK1-mCherry. Images taken every 30 s, over 6 min. Bar = 10 μm. (Ba') Maximum projection of single metaphase cell expressing PLK1-mCherry. Bar = 5 μm. (Bb') 3D surface plot of metaphase cell (from a') displaying PLK1-mCherry integrated intensity measurements ranging between 0 and 250. Spindle poles marked 1 and 2. Fire-LUT (ImageJ). (C) PLK1-mCherry integrated intensity at the highest spindle pole (pole 1) was normalized to 100% and compared with the lowest spindle pole within a single mitotic spindle ($n = 49$ cells measured across 10 embryos ± SEM, Student's t test, $p < 0.0001$). (D) Shown is a single prometaphase cell expressing PLK1-mCherry with poles 1 and 2 marked by a ROI at time point 0 s. PLK1-mCherry integrated intensity is displayed through a Fire-LUT where high intensity white pixels are 35,000 and lower intensity black pixels are 0. The ROIs where PLK1 intensity between poles 1 and 2 is symmetric is highlighted in gray (0 s). Where PLK1 intensity is asymmetric is highlighted in blue (120 s). Bar = 5 μm. (E) Line graph of PLK1 intensity over 2.5 min at poles 1 (magenta) and 2 (cyan) featured in D, illustrating periods of symmetric (gray) and asymmetric (blue) PLK1 intensity between the spindle poles. (F–I) Data from human retinal pigment epithelial (RPE) cells stably expressing GFP-PLK1. (F) Representative images of fluorescence recovery after photobleaching (FRAP) of GFP-PLK1 expressing RPE cells at spindle poles during metaphase (Fire-LUT, ImageJ). Bar = 5 μm. 3D surface plot of a single metaphase cell displaying GFP-PLK1 integrated intensity between the two spindle poles. Spindle poles 1 and 2 are marked. (G) GFP-PLK1 integrated intensity at the highest spindle pole (pole 1) was normalized to 100% and compared with the lowest spindle pole within a single mitotic spindle, over $n = 44$ cells in $n = 3$ experiments ± SEM, Student's paired t test, $p < 0.001$. (H) Model of centrosome-localized PLK1-activity FRET biosensor where active PLK1 phosphorylates the substrate sequence c-jun (green), causing the FHA2 domain (magenta) to bind, and leading to a conformational change in the biosensor and subsequent loss of FRET. Increased phosphatase activity causes the biosensor to enter a relaxed conformation, allowing FRET (Colicino *et al.*, 2018). (I) Quantification of the inverse FRET ratio across multiple spindle poles displayed as a box and whisker plot. Pole 1 binned as mitotic centrosome with highest inverse FRET ratio (gray) compared with pole 2 (blue) from a single mitotic spindle. Representative of FRET ratio at a single mitotic centrosome shown (Fire-LUT, ImageJ). $n = 60$ cells, + indicating mean, and each data point representing a single mitotic centrosome, Student's paired t test, $p < 0.001$.

mitotic spindle, the spindle pole with a higher inverse FRET ratio as spindle pole 1 and the spindle pole with a lower inverse FRET ratio as spindle pole 2. This was done over 60 metaphase cells, where we calculated that one spindle pole (pole 1) had a significantly greater inverse FRET ratio (median of 2.43) compared with the other (pole 2, median of 2.06; Figure 1I). Together, these data suggest that an asymmetry in PLK1 distribution and activity exists between the two spindle poles in metaphase cells.

Chromosome misalignment drives asymmetry in PLK1 distribution

A possible mechanism to respond to misaligned chromosomes is to adjust PLK1 distribution between spindle poles. During prometaphase exit and metaphase, misaligned chromosomes can be found that realign with the metaphase plate (Figure 2A). During these situations, we imaged GFP-PLK1 RPE cells every 2 min across the full volume of the cell until it passed through anaphase (~20 min in duration). GFP-PLK1 intensity was then measured at each spindle

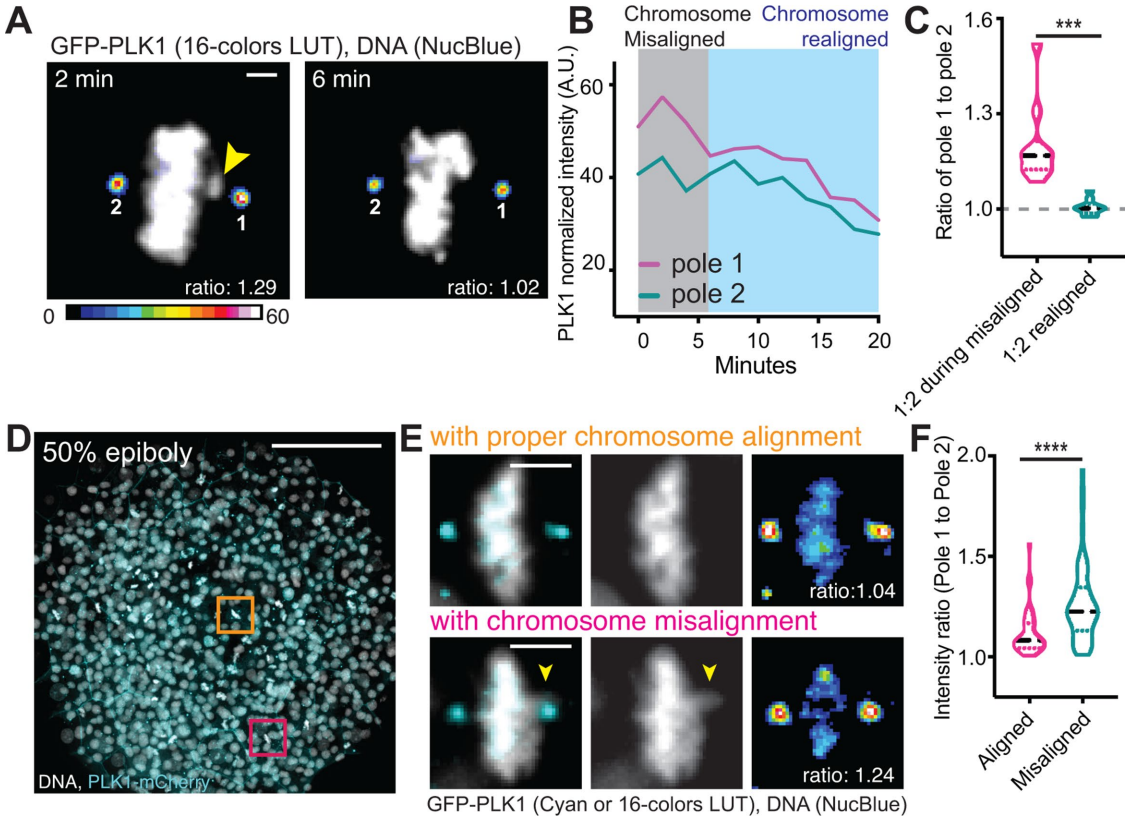

FIGURE 2: PLK1 asymmetric distribution between spindle poles is driven by chromosome misalignment. (A) GFP-PLK1 (16-color LUT, Image J) RPE cells treated with NucBlue to stain DNA (white) were imaged every 2 min. Shown is a time point with a misaligned chromosome (2 min, arrow) that then assembles within the metaphase plate by 6 min. Bar = 2 µm. The spindle pole on the side with the misaligned chromosome is marked as 1, and the opposite pole is 2. Ratio values for GFP-PLK1 between poles 1 and 2 shown in the lower right corner. (B) The intensity of poles 1 and 2 from A was measured over a 20-min time course and plotted. Chromosome misalignment marked on plot. (C) The ratio GFP-PLK1 intensity at the spindle pole (labeled 1) with a misaligned chromosome divided by the GFP-PLK1 intensity of spindle pole without a misaligned chromosome (labeled 2) was measured during misalignment (magenta) and postmisalignment (cyan) in the same cell over $n = 10$ live-cell data sets. Violin plot shown. Dashed line at median; dotted lines at interquartile range. Student's paired t test; ***, $p < 0.001$. (D) Maximum projection of a zebrafish embryo expressing PLK1-mCherry (cyan) and NucBlue (white). Examples of metaphase cells with proper chromosome alignment (orange) and chromosome misalignment (magenta) denoted by boxes. Bar, 100 µm. (E) Example images of mitotic cells from D with proper chromosome alignment (top, orange box in D) and chromosome misalignment (bottom, magenta box in D). PLK1-mCherry (cyan) and NucBlue (white) shown in left and center images. PLK1-mCherry (16-color LUT) in right images to denote areas of high PLK1 intensities. Ratio values for PLK1-mCherry between mitotic spindle poles shown in the top right corner. Bar = 5 µm. (F) Violin plot depicting the ratio between the highest PLK1-intensity spindle pole over the lowest PLK1-intensity spindle pole in mitotic cells with an aligned metaphase plate (magenta) or misaligned (cyan). $n > 45$ cells/treatment across $n = 11$ embryos. Student's paired t test; ****, $p < 0.0001$.

pole over time. The spindle pole with the misaligned chromosome in closest proximity was binned as spindle pole 1 and the other as spindle pole 2. When a misaligned chromosome occurred, spindle pole 1 contained an elevated GFP-PLK1 signal compared with spindle pole 2 (Figure 2, A and B). To examine whether this was a consistent phenomenon, a ratio was calculated for GFP-PLK1 intensity at the spindle pole with a misaligned chromosome (pole 1) over the spindle pole without the misaligned chromosome (pole 2) during time points of misalignment compared with time points postmisalignment over 10 dividing cells (Figure 2C). During misalignment, a mean ratio of 1.33 occurs compared with postmisalignment where a mean ratio is at 1.01 (Figure 2C), suggesting that asymmetry in PLK1 between mitotic spindle poles is due to adjustments in chromosome alignment.

Next, we tested whether this occurs in vivo by examining division in a zebrafish embryo expressing PLK1-mCherry and chromosomes stained with 4′,6-diamidino-2-phenylindole (DAPI) or NucBlue. In a fixed, 50% epiboly embryo (Figure 2D), we noted metaphase cells with misaligned chromosomes compared with cells with a clearly aligned metaphase plate (Figure 2E). Under these conditions, we calculated a ratio of the spindle pole with highest intensity over the pole with lowest intensity and determined that the mean ratio is significantly higher under conditions of misaligned chromosomes (mean at 1.27) compared with dividing cells with an aligned plate (mean at 1.12; Figure 2F). Taken together, these studies suggest that chromosome misalignment is causing an elevated asymmetric distribution of PLK1 at spindle poles both in tissue culture and in vivo.

Determining oldest from youngest mitotic spindle pole and PLK1 distribution between the two

Chromosomes preferentially misalign toward the oldest spindle pole, the one containing the oldest mitotic centriole (Gasic *et al.*, 2015). In our studies, we utilized HeLa cells that stably express GFP-centrin to

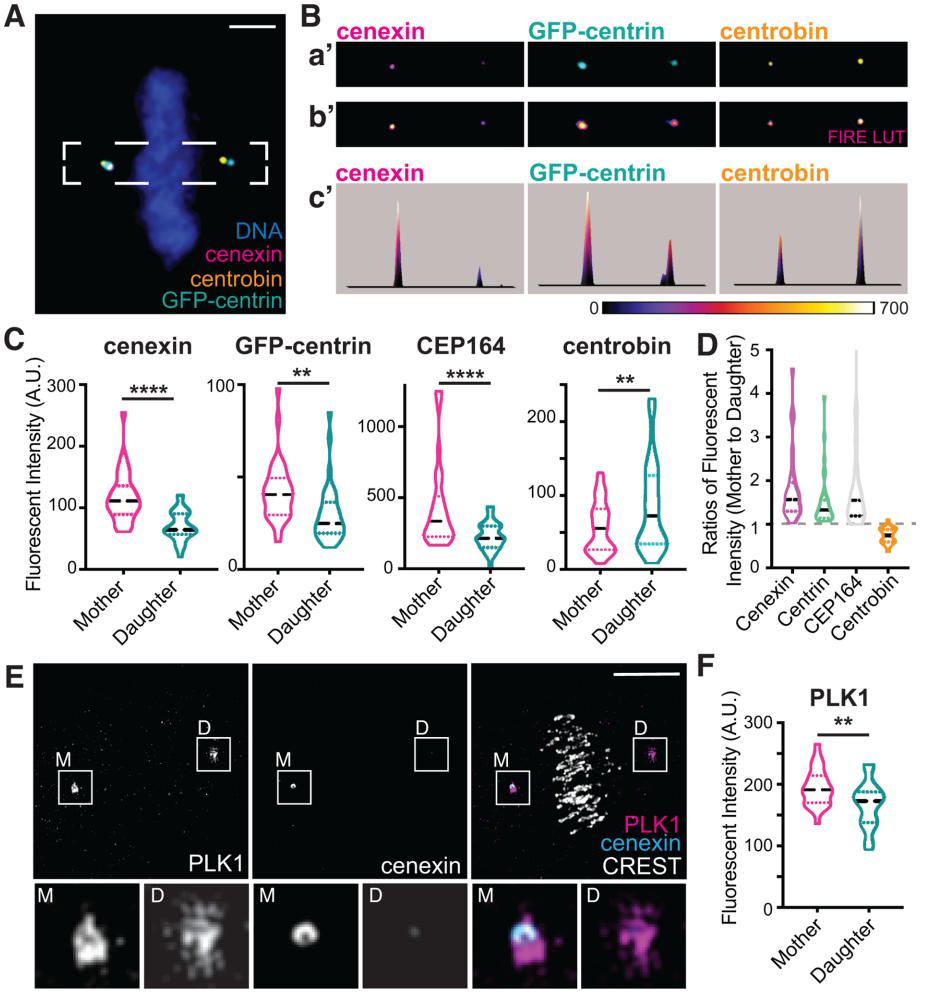

FIGURE 3: PLK1 distribution between the oldest (mother) and youngest (daughter) spindle poles. (A) Immunofluorescence staining of HeLa GFP-centrin cells at metaphase, centrioles (centrin, cyan), cenexin (magenta), centrobin (gold), and DNA (blue). Bar = 3 μm. (B) Insets from A showing cenexin (magenta), GFP-centrin (cyan), and centrobin (gold; Ba'). Fire-LUT depicting intensities of cenexin, GFP-centrin, and centrobin (Bb'). 3D profile plot of each pole. Heat map of intensity ranges (Bc'). (C) The intensity of cenexin, GFP-centrin, CEP164, and centrobin was measured at the mother and daughter spindle pole. Violin plot shown, black dashed line at median. Representative of $n = 3$ experiments, $n > 30$ cells measured/group. Student's paired t test; **, $p < 0.01$; ****, $p < 0.0001$. (D) Measured fluorescence intensities were used to calculate a ratio for each metaphase cell where the mother spindle pole intensity was divided by that of the daughter spindle pole. Violin plot shown, black dashed line at median. Representative of $n = 3$ experiments, $n > 30$ cells/group. (E) Structured illumination micrograph (SIM) volumetric projection of a single metaphase HeLa cell immunolabeled for PLK1 (magenta), cenexin (cyan), and CREST (gray). Mother spindle pole (M) and daughter spindle pole (D). White insets depict single mitotic centrosomes. Bar = 5 μm. (F) PLK1 fluorescence intensity was measured at the mother and daughter spindle pole (determined by GFP-centrin) across $n = 30$ cells. Violin plot shown, black dashed line at median. Student's paired t test; **, $p < 0.01$.

distinguish mother from daughter spindle poles. GFP-centrin is enriched at the oldest spindle pole (mother) compared with the youngest spindle pole (daughter) due to the nature of centriole duplication. When new protein synthesis of centrin occurs, new centrioles incorporate freshly translated centrin. Thus, the oldest centriole has more centrin accumulated (Piel *et al.*, 2000; Wang *et al.*, 2009; Kuo *et al.*, 2011). Additional markers used to distinguish between the oldest and youngest pole were two mother centriole appendage proteins, cenexin (a subdistal appendage protein; Ishikawa *et al.*, 2005; Hehnly *et al.*, 2012; Hung *et al.*, 2016) and CEP164 (a distal appendage protein; Schmidt *et al.*, 2012; Hung *et al.*, 2016), along with the daughter centriole protein centrobin (Januschke *et al.*, 2011; Hehnly *et al.*, 2015). When a single centrosome duplicates to two spindle poles, one spindle pole will inherit the mother centriole, while the other spindle pole does not (Hung *et al.*, 2016; Vertii *et al.*, 2018). The oldest mitotic centriole is positive for cenexin and CEP164 and is enriched for GFP-centrin (Figure 3, A–C, and Supplemental Figure 2, A and B). The youngest spindle pole has elevated amounts of the daughter centriole marker, centrobin (Figure 3, A–C; Hehnly *et al.*, 2015). We then calculated a ratio between mother and daughter spindle poles of CEP164, cenexin, GFP-centrin, and centrobin. In these studies the mother was distinguished by its elevated amounts of GFP-centrin (Piel *et al.*, 2000; Wang *et al.*, 2009; Kuo *et al.*, 2011). CEP164, cenexin, and centrin were enriched on the mother (ratios >1; an equal distribution of 1 is at the dashed line), whereas centrobin was enriched on the daughter (ratio <1; Figure 3D).

Cenexin has been identified to interact with PLK1 (Soung *et al.*, 2006, 2009). Using structured illumination microscopy (SIM) we found that cenexin was organized on one spindle pole (mother, M) in a specific "ring-like" pattern, and PLK1 organized in a similar pattern (Figure 3E). This finding suggests that cenexin may be organizing a population of PLK1 specifically on one of the two spindle poles. When we measured the integrated fluorescence intensity of endogenous PLK1 at mother and daughter spindle poles in HeLa GFP-centrin cells, we found that the mother spindle pole (the one with the most GFP-centrin) contained significantly more PLK1 than the daughter spindle pole (Figure 3, E and F).

PLK1 activity increases at the oldest spindle pole when a lagging chromosome is in close proximity

We measured PLK1 activity at spindle poles in cells expressing the centrosome-localized PLK1 activity FRET-biosensor (Figure 1H; Colicino *et al.*, 2018). We did these studies with nocodazole synchronized and released cells under fixed conditions so that we could analyze more cells and induce misaligned chromosomes (Crasta *et al.*, 2012). Cells were fixed so that mother and daughter spindle poles could be distinguished, and kinetochores visualized. To identify the mother and daughter spindle poles, we used the molecular marker centrobin (Figure 3, B–D) or centrin (Supplemental Figure 2B). Kinetochores were denoted by immunostaining for CREST. We measured PLK1 activity under conditions of normal chromosome alignment, misaligned chromosomes toward the mother spindle pole, or misaligned chromosomes toward the daughter spindle pole (Figure 4A). Misaligned chromosomes were determined by identifying kinetochores outside the metaphase plate (yellow arrowheads in Figure 4A). These unaligned

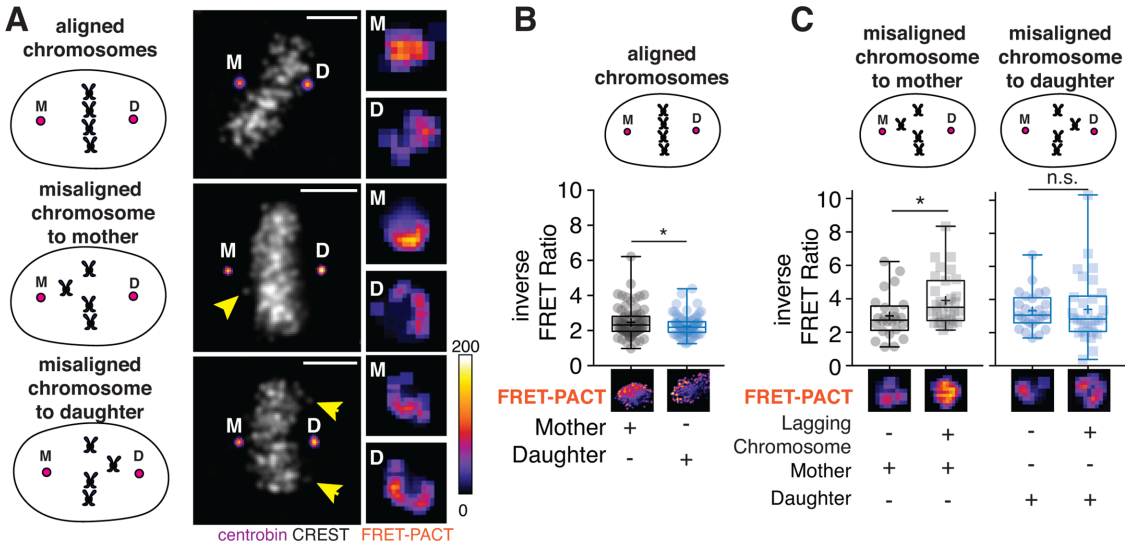

FIGURE 4: PLK1 activity increases at the oldest spindle pole (mother) when a misaligned chromosome is in close proximity. (A) Models depicting conditions of normal chromosome alignment (top), misaligned chromosome to the mother spindle pole (center), and misaligned chromosome to the daughter spindle pole (bottom). Representative maximum confocal projections of metaphase HeLa cells immunostained for centrobin (magenta) and DAPI (white). Insets show inverse FRET ratio of the PLK1-FRET biosensor (right, Fire-LUT; ImageJ). The mother (M) and daughter (D) spindle poles labeled respectively. Bars = 5 μm. (B) Significantly greater PLK1 activity FRET ratios are measured at the mother (gray) spindle pole compared with the daughter (blue) under conditions of normal chromosome alignment. $n = 79$ cells over $n = 3$ experiments. Data shown as a box and whisker plot, + indicating mean, and each data point representing a single spindle pole. Student's paired t test, $p = 0.0139$. (C) Greater PLK1 activity FRET ratios are measured at the mother (gray) spindle pole when there is a misaligned chromosome in close proximity, but no change in PLK1 activity is measured when chromosomes misalign toward the daughter (blue). $n > 20$ cells over $n = 3$ experiments, data shown as a box and whisker plot, + indicating mean, and each data point representing a single spindle pole. Student's unpaired t test, lagging chromosomes to mother ($p = 0.0022$), lagging chromosomes to daughter ($p = 0.7044$).

chromosomes were positive for the mitotic kinase Aurora B (Supplemental Figure 2C). Aurora B is at its highest concentration between two sister chromatids when misaligned chromosomes are not under appropriate tension (Lampson and Cheeseman, 2011). Under conditions of normal chromosome alignment, a slight yet significant increase in PLK1 activity was measured at the mother spindle pole (median of 2.32) compared with the daughter (median of 2.19; Figure 4B). We next compared PLK1 activity at the mother spindle pole with and without a misaligned chromosome (Figure 4C, left) to the PLK1 activity at the daughter pole with and without a misaligned chromosome (Figure 4C, right). In the event of a misaligned chromosome toward the mother, PLK1 activity measured significantly higher (median of 3.50) compared with conditions where there were no detectable misaligned chromosomes (Figure 4C, left). In the event of a misaligned chromosome at the daughter spindle pole, there was no significant difference in PLK1 activity (Figure 4C, right). From this, we conclude that PLK1 activity can increase at the oldest spindle pole specifically when a chromosome misaligns in that direction.

An increase in PLK1 activity at the mother spindle pole is cenexin dependent

To determine whether an increase in PLK1 activity at the mother spindle pole in the event of a lagging chromosome is cenexin-dependent, we utilized a previously published cenexin-depleted HeLa cell line (Hung *et al.*, 2016). Immunostaining (Figure 5, A and B) and immunoblotting (Figure 5C) confirmed cenexin depletion by short hairpin RNA (shRNA). We noted that in control shRNA–treated cells, 24.98 ± 3.83% of their mitotic cells presented with misaligned chromosomes, whereas in cenexin shRNA–treated cells, this percentage significantly increased to 39.3 ± 4.00% (Figure 5, A and D, refer to arrow, and Table 1).

We next examined cells synchronized in metaphase using the anaphase promoting complex inhibitor, ProTAME (10 μM), or the microtubule destabilizing drug, nocodazole (100 nM). In control cells treated with ProTAME, 19.93 ± 4.45% of mitotic cells had misaligned chromosomes (Figure 5D and Table 1). In ProTAME synchronized cenexin-depleted cells there was a threefold increase compared with control (64.9 ± 10.60%; Figure 5D and representative images in Supplemental Figure 2D). The misalignment observed in ProTAME synchronized cells was severe with misaligned chromosomes accumulating at both poles (Supplemental Figure 2D). A similar increase in the percentage of mitotic cells with misaligned chromosomes was observed in cenexin-depleted cells synchronized in nocodazole (48.47 ± 5.40%) when compared with controls (38.80 ± 6.28%; Table 1). Together these studies suggest that cenexin loss is causing defects in chromosome alignment.

We next tested whether cenexin localization at the mother spindle pole drives preferential distribution of PLK1 activity. The centrosome-localized PLK1 FRET activity biosensor was expressed in cenexin-depleted HeLa cells. These studies were performed under fixed conditions with cells that were nocodazole synchronized and released. Under conditions of normal chromosome alignment, there was no significant difference in the inverse FRET ratios between the mother (median of 2.184) and daughter spindle pole (median of 2.16; Figure 5E). When a misaligned chromosome was present toward the mother spindle pole, there was no significant increase in PLK1 activity at this site (Figure 5F, left). Additionally, there was no increase in PLK1 activity at the daughter when a misaligned chromosome was present (Figure 5F, right). To directly

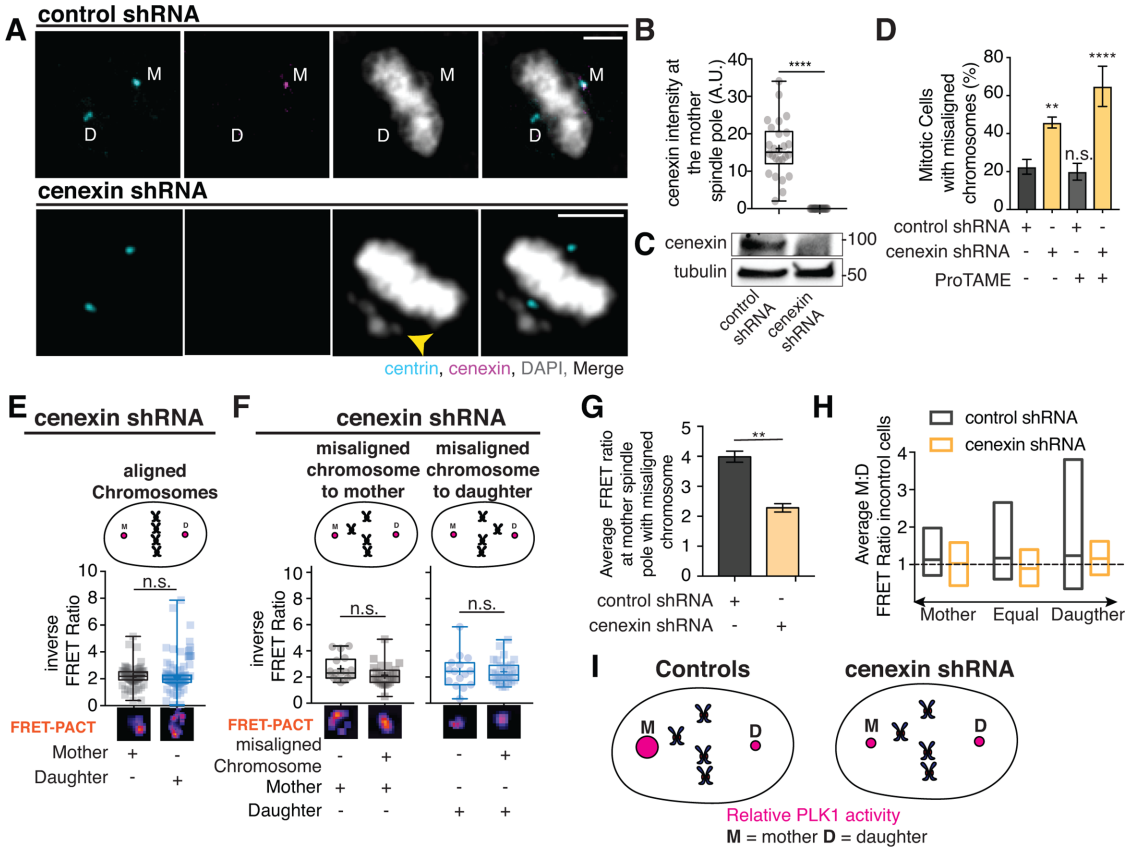

FIGURE 5: An increase in PLK1 activity at the oldest spindle pole (mother) in the event of a misaligned chromosome is cenexin dependent. (A) Maximum confocal projections of control shRNA and cenexin shRNA HeLa cells immunostained for centrin (cyan), cenexin (magenta), and DAPI (gray). Yellow arrowhead indicates misaligned chromosomes. Bars = 5 μm. (B) Cenexin fluorescence intensity at the mother spindle pole in control shRNA and cenexin shRNA HeLa cells. Data shown as a box and whisker plot over $n > 26$ cells, + indicating mean, and each data point representing a single spindle pole. Representative from $n = 3$ experiments. Student's t test, $p < 0.0001$. (C) Western blot of HeLa cells expressing a control nontargeting shRNA or a cenexin shRNA. Tubulin loading control shown below. (D) Bar graph depicting percent (%) metaphase cells with misaligned chromosomes in control and cenexin-depleted cells under control conditions or after ProTAME (10 μM) synchronization in metaphase. $n = 3$ experiments ± SEM. With a one-way ANOVA applying multiple comparisons to control shRNA, cenexin shRNA-treated (**, $p = 0.0023$) and cenexin shRNA-treated plus ProTAME (****, $p < 0.0001$) are significant. (E) PLK1 activity FRET ratios between the mother (gray) and daughter (blue) spindle poles in cenexin-depleted cells when chromosomes are properly aligned. $n > 80$ cells over $n = 3$ experiments, data shown as a box and whisker plot, + indicating mean, and each data point representing a single spindle pole. Student's paired t test, $p = 0.3504$. (F) PLK1 activity in cenexin-depleted cells in the presence of a misaligned chromosome toward the mother (gray) spindle pole or the daughter (blue) spindle pole. $n > 40$ cells over $n = 3$ experiments, data shown as a box and whisker plot, + indicating mean, and each data point representing a single spindle pole. Student's unpaired t test, misaligned chromosome to mother ($p = 0.0719$), misaligned chromosome to daughter ($p = 0.9415$). (G) Bar graph representing average PLK1 FRET ratio at the mother spindle pole in cenexin-depleted cells compared with controls in the event of a misaligned chromosome toward the mother spindle pole across $n = 3$ experiments ± SEM, Student's t test, $p = 0.0018$. (H) Ratio of PLK1 FRET between the mother and daughter (FRET ratios at mother/FRET ratios at daughter) were compared in control cells (gray) and cenexin-depleted cells (gold) under conditions of equal chromosome misalignment toward both spindle poles, asymmetry in misaligned chromosomes toward the mother spindle pole, or asymmetry in misaligned chromosomes toward the daughter spindle pole. Black dotted line at $y = 1$ represents equal FRET ratios between mother and daughter spindle poles. $n > 56$ cells in graph measured over $n = 3$ experiments. Range of data shown as a box plot; center bar represents mean. (I) Model illustrating an increase in PLK1 activity (magenta) in control cells, which does not occur in cenexin-depleted cells.

compare the differences in activity at the mother spindle pole when a misaligned chromosome is present in cells treated with control shRNA or cenexin shRNA, the average inverse FRET ratios for PLK1 were calculated over $n = 3$ experiments. A significantly higher average inverse FRET ratio was calculated in control cells (3.99 ± 0.19) compared with cenexin-depleted cells (2.28 ± 0.14; Figure 5G). These studies suggest a mechanism where PLK1 activity at the oldest spindle pole can respond to chromosome misalignment in a cenexin-dependent manner. If cenexin is absent, an increase in overall misalignment occurs (Figure 5D and Table 1).

We examined how PLK1 activity was distributed between the two spindle poles when more than one chromosome misaligns. The inverse FRET ratio at the mother spindle pole and the inverse FRET ratio at the daughter spindle pole were calculated and presented as a mother to daughter ratio (M:D). If there are consistently equal activities between the two spindle poles, a tight range of values that

	% metaphase cells with misaligned chromosomes	% of misaligned metaphase cells with chromosomes toward mother	% of misaligned metaphase cells with chromosomes toward both poles
Control shRNA	24.98 ± 3.83	58.08 ± 4.28	20.10 ± 5.32
Control shRNA+ 100 nM nocodazole	38.88 ± 6.28	57.49 ± 11.79	24.75 ± 11.81
Control shRNA+ 10 μM ProTAME	19.93 ± 4.45	56.79 ± 4.90	18.55 ± 12.01
Control shRNA+ 100 nM BI2536	44.63 ± 3.70	41.42 ± 0.72	36.48 ± 3.20
Cenexin shRNA	39.3 ± 4.00	42.9 ± 2.80	31.37 ± 1.90
Cenexin shRNA+ 100 nM nocodazole	48.47 ± 5.40	16.86 ± 0.90	65.45 ± 4.90
Cenexin shRNA+ 100 nM BI2536	61.00 ± 3.40	54.33 ± 5.21	18.07 ± 3.36

The mitotic index, percent of mitotic cells that had chromosomes misaligned toward the mother spindle pole, and the percent of mitotic cells that had chromosomes misaligned toward both spindle poles are shown. These measurements were completed for control shRNA HeLa cells as well as cenexin shRNA HeLa cells treated with 100 nm of nocodazole, 10 μm of ProTAME, or 100 nm of BI2536. Percentages are mean percentages over $n > 3$ experiments ± SEM.

TABLE 1: Cenexin and PLK1 regulate directional chromosome misalignment during metaphase.

organize around 1 should be calculated. The ratios presented were calculated under three different conditions: 1) when chromosome misalignment was equal to each pole (e.g., one chromosome toward the daughter and one chromosome toward the mother); 2) asymmetric mother misalignment (e.g., >2 chromosomes toward the mother and <2 chromosomes toward the daughter), and asymmetric daughter misalignment (e.g., <2 chromosomes toward the mother and >2 chromosomes toward the daughter). In control cells, we found a range in activity that always trends above 1 under all conditions. However, in cenexin-depleted cells, a tighter trend that concentrated around a value of 1 was calculated (Figure 5H). This graph suggests that in control cells under both symmetric and asymmetric chromosome misalignment conditions, there is a bias in PLK1 activity toward the mother spindle pole. This bias is lost, however, when cenexin is depleted (Figure 5H). From here, we present a model where PLK1 acts as a sensor to correct for chromosome misalignment at the cenexin-positive oldest spindle pole (mother; Figure 5I).

Chromosomes predominately misalign toward the oldest spindle pole in a cenexin- and PLK1-dependent manner

A previous report demonstrated an inherent bias for chromosomes to preferentially misalign toward the oldest spindle pole (mother) in a cenexin-dependent manner (Gasic *et al.*, 2015). This suggests a reason for a sensing mechanism to be in place specifically at the mother spindle pole. To confirm and expand upon the findings of Gasic *et al.* (2015), we utilized control and cenexin-depleted HeLa cells stably expressing GFP-centrin (to determine centrosome age; Figure 3, A–D, and Supplemental Figure 3, A and B; Piel *et al.*, 2000; Kuo *et al.*, 2011) and mCherry-CENPA (to follow chromosome missegregation by marking kinetochores; Posch *et al.*, 2010; Gasic *et al.*, 2015). The number of chromosomes (marked by mCherry-CENPA) that misaligned were evaluated by live-cell video microscopy (Supplemental Figure 3, C and D, and Supplemental Video 3). We found a preferential directionality in misaligned chromosomes toward the mother (53.7%), compared with the daughter (19.5%), and toward both spindle poles (26.8%; Supplemental Figure 3C). Notably, we found that anywhere between 1 and 6 chromosomes can misalign toward the mother, whereas ≤2 chromosomes tend to misalign toward the daughter under control conditions (Supplemental Figure 3C). These studies were confirmed over four experiments where 54.17 ± 6.59% of cells presented with preferential chromosome misalignment toward the mother (Supplemental Figure 3D). However, this preferential misalignment is disrupted in cells where cenexin is depleted by shRNA (Supplemental Figure 3D). Together, the results suggest that chromosomes preferentially misalign toward the oldest spindle pole in a cenexin-dependent manner.

Because chromosomes preferentially misalign toward the oldest spindle pole (mother), and PLK1 activity is significantly increased at the mother in the presence of misaligned chromosomes, it is possible that directional chromosome misalignment occurs in a PLK1- and cenexin-dependent manner. To test this, we treated both control and cenexin-depleted cells with the PLK1 inhibitor, BI2536 (100 nM), fixed, and then scored metaphase cells that had misaligned chromosomes toward the mother, daughter, or both spindle poles (Figure 4A). In control cells, chromosomes tend to misalign toward the mother (58.08 ± 4.28% of cells; Figure 6, B and C, and Table 1). This preferential misalignment occurs under two methods of synchronization, either with 100 nM nocodazole followed by 20–30 min release (57.49% ± 11.79% mitotic cells misalign chromosomes toward the mother) or using 10 μM of ProTAME (56.79 ± 4.90% mitotic cells misalign chromosomes toward mother; Table 1). However, there was a significant decrease in the percentage of cells that misalign chromosomes toward the mother in cenexin-depleted cells (39.30 ± 4.00%; Figure 6, B and C, and Table 1), with an increase to both spindle poles (31.37 ± 1.90%, compared with controls at 20.10 ± 5.32%; Figure 6, B and C, and Table 1). With PLK1 inhibition (100 nM BI2536), the percentage of cells with preferential chromosome misalignment toward the mother significantly dropped to 44.63 ± 3.70% (Figure 6, B and C, and Table 1). These studies suggest that either PLK1 inhibition (BI2536 treatment), or cenexin depletion, causes an increased probability for chromosomes to misalign toward both spindle poles compared with just the mother.

To test whether PLK1 and cenexin might be acting together to modulate the direction of chromosome misalignment, we treated cenexin-depleted cells with the PLK1 inhibitor BI2536 and compared with control shRNA–treated cells, cells treated with BI2536 alone, and cenexin shRNA–treated cells. Strikingly, in cells treated with both cenexin shRNA and BI2536, cells are restored to control conditions, with 54.33 ± 5.21% of mitotic cells with misaligned chromosomes going toward the mother and only 18.07 ± 3.36% of cells with misaligned chromosomes toward both spindle poles (Figure 6, B and C, and Table 1). Of note, under these conditions 61 ± 3.40% of the total population of metaphase cells have misaligned chromosomes compared with BI2536- (44.63 ± 3.70%) or cenexin shRNA–treated (39.3 ± 4.0%; Table 1) cells.

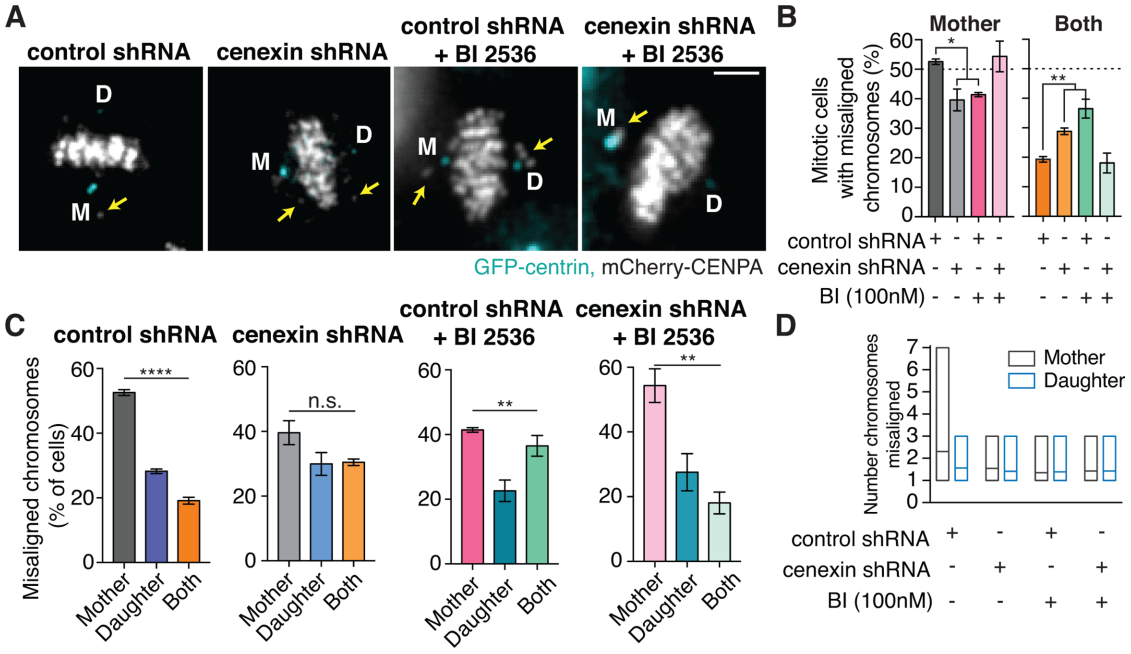

FIGURE 6: Chromosomes predominately misalign toward the oldest spindle pole in a PLK1- and cenexin-dependent manner. (A) Maximum confocal projections of HeLa cells stably expressing centrin-GFP, CENPA-mCherry, and either a control or cenexin shRNA, treated with 100 nM BI2536. Yellow arrows depict lagging chromosomes. Bar = 5 μm. (B) Bar graph quantifying percentage of cells that display misaligned chromosomes toward the mother spindle pole (left) or both spindle poles (right) in control and cenexin-depleted cells ± 100 nM BI2536 treatment. Dotted line at 50% represents randomization. $n = 3$ experiments ± SEM, one-way ANOVA (*, $p = 0.0131$; **, $p = 0.0028$). (C) Quantification of misaligned chromosome directionality (%) in control and cenexin-depleted HeLa cells ± 100 nM BI2536 treatment. $n > 50$ cells over $n = 3$ experiments ± SEM; a one-way ANOVA was performed for each condition: control shRNA ($p < 0.0001$), cenexin shRNA ($p = 0.1099$), control shRNA +BI ($p = 0.0063$), cenexin shRNA +BI ($p = 0.0047$). (D) Number of individual misaligned chromosomes toward either the mother (gray) or daughter (blue) spindle poles under conditions where chromosomes misalign in both directions. $n > 5$ experiments, range of data shown as a box plot, and center bar represents mean.

To test whether there is a bias under conditions where there is chromosome misalignment toward both spindle poles, the number of chromosomes toward the mother and daughter were scored per cell (Figure 6D). Control cells presented with a tendency for more chromosomes to misalign toward the mother spindle pole (anywhere from one to seven chromosomes, noted by CREST staining) compared with the side of the cell with the daughter (one to three chromosomes; Figure 6D). This trend toward the mother, however, is diminished when cells are treated with a cenexin shRNA, BI2536, or both cenexin shRNA and BI2536. Under these conditions, there is equal chromosome segregation to both sides of the spindle (anywhere from one to three chromosomes). This result suggests that, even under conditions of chromosome misalignment toward both spindle poles, there is still a bias for chromosomes to misalign toward the oldest spindle pole in a cenexin- and PLK1-dependent manner.

DISCUSSION

Through this study, we determined that if chromosomes misalign, these chromosomes are more likely to misalign toward the oldest spindle pole (mother). Upon misalignment toward the mother, one cellular response that occurs is a cenexin-dependent increase in PLK1 activity at this site. On the basis of this result, we present a model where cenexin and PLK1 work together in response to misaligned chromosomes. We propose this model based on the known interaction between PLK1 and cenexin (Soung *et al.*, 2006, 2009), and our studies that identified PLK1 in a ring-like structure at the mother spindle pole colocalizing with the ring-like structure cenexin forms (Figure 3E). Additionally, we find that PLK1 inhibition or cenexin depletion causes chromosomes to no longer preferentially misalign toward the mother (Figure 6, A–C, and Table 1). Instead, chromosomes tend to misalign more toward both spindle poles (Figure 6, B and C, and Table 1). However, if we combine PLK1 inhibition with cenexin depletion, we restore the propensity for chromosomes to misalign toward the mother (Figure 6, B and C, and Table 1), but cause an increased percentage of mitotic cells to have misaligned chromosomes (61.00 ± 3.40% compared with cenexin depletion at 39.3 ± 4.0%). From these studies we propose a model that PLK1 and cenexin work together as a sensor to correct and respond to chromosome misalignment.

Another potential model is that the mother spindle pole is driving chromosomes to misalign toward itself and is not necessarily acting as a sensor to fix a misaligned chromosome. If this were the case, we would propose that depleting cenexin would decrease chromosome misalignment toward the mother, but not affect overall chromosome misalignment. Here, we find that cenexin depletion significantly decreases chromosome misalignment toward the mother spindle pole (Figure 6B and Table 1), but causes a subsequent increase in the total percentage of cells that present with misaligned chromosomes toward both spindle poles (Figure 6, B and C, and Table 1). We did not find a condition that preferentially forced chromosomes to misalign toward the daughter spindle

pole. These data support our first proposed model that PLK1 and cenexin work as a sensor to respond to and fix chromosome misalignment.

We predict that in order for PLK1 and cenexin to act as a sensor to fix misaligned chromosomes, a feedback mechanism needs to be in place to alert the spindle pole to a misaligned chromosome in close proximity. Active PLK1 resides at the kinetochore of misaligned chromosomes, acting as a mitotic checkpoint until proper microtubule attachments have been made and the error has been rectified (Liu *et al.*, 2012). To date, distinct, independent pools of active PLK1 have not been identified between spindle poles and kinetochores. This leaves the potential for active-PLK1 to cross-communicate or exchange between the kinetochores and centrosomes, alerting the oldest spindle pole of a misaligned chromosome. This would allow the spindle pole closest to the lagging chromosome to become hyperactivated through increased PLK1 activity. This increase in PLK1 activity could potentially recruit more PCM components to nucleate more microtubules to correct the misaligned chromosome. PLK1 activity has been associated with recruiting PCM proteins such as pericentrin, CEP215, and γ-tubulin (Lee and Rhee, 2011; Kong *et al.*, 2014; Ramani *et al.*, 2018). Each of these components is also known to be enriched at the oldest spindle pole and CEP215 and pericentrin form a complex with the mother centriole appendage protein, centriolin (Conduit and Raff, 2010; Conduit *et al.*, 2010; Chen *et al.*, 2014). Thus, increased PLK1 activity specifically at the mother spindle pole can lead to pericentriolar material remodeling specifically at this spindle pole.

Our finding that a bias exists in chromosome misalignment toward the mother spindle pole may have evolutionary implications. For instance, previous studies have determined using the *Drosophila* germline that the mother spindle pole is inherited by the daughter cell that remains stem, while the daughter spindle pole is inherited by the cell destined for differentiation (Yamashita *et al.*, 2007). When stem cells divide, these divisions are responsible for repopulating the stem-cell niche, as well as providing cells that will differentiate. This preference for the mother to be inherited by the cell which remains within the stem cell population could shed light on why the oldest spindle pole preferentially misaligns chromosomes during division. Stem cells are better equipped to cope with aneuploidy compared with differentiated cells (reviewed in Garcia-Martinez *et al.*, 2016), due to the importance of these cells in maintaining genome integrity. To combat aneuploidy, stem cells have multiple forms of defense. These defenses include increased expression of DNA damage repair (DDR), which can repair the genomic errors associated with aneuploidy (Maynard *et al.*, 2008) and p53-driven apoptosis or spontaneous differentiation, which removes the aneuploid cell from the stem cell population to retain genomic integrity (Jain *et al.*, 2012). An alternative viewpoint in this argument is that stem cells provide an opportunity to pass on "cultural adaptations" that may arise as the result of aneuploidy (Enver *et al.*, 2005). This would allow stem cells to develop an advantage due to this new, unique genome, allowing for adaptations in differentiated cells previously unavailable. Together, this could explain why our studies showed a preferential, directional misalignment of chromosomes toward the mother.

In conclusion, our studies utilize both a zebrafish embryonic model and an in vitro cell culture model to demonstrate an asymmetry in PLK1 distribution and activity between the two spindle poles. Here, we argue that this asymmetry is conserved and occurs predominately during instances of chromosome misalignment toward the mother spindle pole.

MATERIALS AND METHODS

Antibodies and chemical inhibitors

For Western blot analysis and immunofluorescence imaging, the following antibodies were used: mouse anti-PLK1 (E-2; Santa Cruz; sc-55504; 1:250), rabbit anti-cenexin (Proteintech; 12058-1-AP; 1:250), mouse anti–α-tubulin monoclonal antibody (Proteintech; 66031-1-Ig; 1:10,000), human anti-CREST (Antibodies; 15-234-0001; 1:1000), mouse anti-centrin clone 20H5 (Millipore Sigma; 04-1624; 1:1000), rabbit anti-CEP164 (Novus Biologicals; NBP1-81445; 1:50), and mouse anti-centrobin (Abcam; ab70448; 1:500). Horseradish peroxidase (HRP)-conjugated antibodies: donkey anti-mouse immunoglobulin G (IgG) (H+L; Jackson ImmunoResearch Labs; 715-035-150), donkey anti-rabbit IgG (H+L; Jackson ImmunoResearch Labs; 711-035-152), and mouse anti-GAPDH (1:10,000, Sigma Aldrich; 45-9295). Fluorescent secondary antibodies include Alexa Fluor donkey anti–mouse 488 (Life Technologies; A21202), 568 (Life Technologies; A10037), and 647 (Life Technologies; A31571); Alexa Fluor donkey anti–rabbit 488 (Life Technologies; A21206), 568 (Life Technologies; A10042), 647 (Life Technologies; A31573), rhodamine-conjugated donkey anti-human (Jackson Immunoresearch; 709-025-149), and DyLight 649-conjugated goat anti-human (Jackson Immunoresearch; 109-495-064). Chemical inhibitors include nocodazole used on cells at 100 nM (Fisher; AC358240500), ProTAME (Fisher; I44001M) used on cells at 10 µM, and BI2536 (Selleck Chemicals; S1133-5 mg) used on cells at 100 nM.

Zebrafish

Zebrafish embryos (provided by Jeffrey Amack's laboratory, SUNY Upstate Medical University) were injected with 100–150 pg PLK1-mCherry mRNA immediately following fertilization. Injected zebrafish were then grown at 30°C until 4.5 h postfertilization. For live imaging, embryos were mounted in MatTek dishes using 2% agar and imaged at 30°C. For fixed imaging, embryos were fixed at 4.5 hpf in 4% paraformaldehyde (PFA) + 0.5% Triton X-100 overnight at 4°C. The following day, embryos were washed in phosphate-buffered saline (PBS) + 0.5% Tween for 20 min, dechorionated, and placed in NucBlue fixed cell stain from Ready Probes (Thermo Fisher Scientific; R37606) for 30 min before imaging.

Cell culture

HeLa cells expressing either control or cenexin shRNA (Hung *et al.*, 2016) and PLK1-GFP RPE cells were used throughout this study. For live-cell imaging, a GFP-centrin/ mCherry-CENPA HeLa cell line was used, a kind gift from Patrick Meraldi, Department of Cell Physiology and Metabolism, Université de Genève (Gasic *et al.*, 2015). All cultures were grown in 1X DMEM (Life Technologies) supplemented with 10% Seradigm FBS (VWR) and 1% penicillin–streptomycin (10,000 U/ml; Life Technologies) and maintained at 37°C with 5% CO_2. Cells were synchronized as noted with either nocodazole (100 nM) or ProTAME (10 µM). For nocodazole synchronization, cells were incubated for at least 6 h in nocodazole to synchronize in prometaphase and then washed with fresh media three times and incubated for 20 min for cells to synchronize in metaphase. With ProTAME synchronization, cells were incubated for 6 h and then immediately fixed.

shRNA and plasmid constructs

Control shRNA and cenexin shRNA (Hung *et al.*, 2016) were infected in HeLa cells stably expressing GFP-centrin and mCherry-CENPA to create a stable cenexin-depleted cell line. Lentiviruses used to generate the stable cell lines used the protocol of Hung *et al.* (2016). FRET experiments were performed using a centrosome-localized

PLK1 FRET-biosensor. This previously characterized biosensor was localized to the centrosome through fusion to the PACT domain (Colicino *et al.*, 2018). pCS2-PLK1-mCherry constructs were generated and verified through sequencing.

Immunofluorescence 2D cultures

Cells were plated on #1.5 coverslips until they reached 90% confluence, and fixed using either methanol (–20°C; described in Colicino *et al.*, 2018) or 4% PFA containing 0.5% Triton X-100 at room temperature for 30 min. Cells were washed, blocked with PBSΔT (PBS, 1% bovine serum albumin, 0.5% Triton X-100), and incubated with primary antibodies for 1 h at room temperature. Cultures were washed three times with PBSΔT and incubated with secondary antibodies for 1 h at room temperature. Coverslips were rinsed with diH_2O and mounted on glass slides using either Vectashield (Vector Laboratories; H-1000) or Prolong Diamond with DAPI mounting media (Thermo Fisher Scientific; P36971).

FRET

HeLa cells expressing either control or cenexin shRNA (Hung *et al.*, 2016) were transfected with PLK1 FRET-PACT sensor using Mirus Bio TransIT-X transfection reagent. After 48 h, cells were treated with 100 nM nocodazole and synchronously released into metaphase after 6 h to induce lagging chromosomes. Cells were imaged live or then fixed using 4% PFA containing 0.5% Triton X-100 at room temperature for 30 min. Cells were immunostained for centrobin (1:500) or centrin (1:1000) to distinguish between the spindle poles and CREST (1:1000) to visualize kinetochores. Coverslips were then mounted in vectashield and imaged using a Leica DMi8 STP800 (Leica, Bannockburn, IL) equipped with an 89 North–LDI laser, Photometrics Prime-95B camera, Crest Optics: X-light V2 Confocal Unit spinning disk, using a HC PL APO 63×/1.40 NA oil CS2 objective. For these experiments, $YFP^{ex}\rightarrow YFP^{em}$ control images were taken, using a 520-excitation laser. $CFP^{ex}\rightarrow YFP^{em}$ was imaged using a 445-excitation laser. The $YFP^{ex}\rightarrow YFP^{em}/CFP^{ex}\rightarrow YFP^{em}$ FRET ratio was calculated using ImageJ Ratio-Plus plug-in after background subtraction and averaged over multiple cells. Experiments were repeated multiple times with similar results.

Imaging

Zebrafish and tissue culture cells were imaged using a Leica SP8 scanning confocal microscope (Leica, Bannockburn, IL) or a Leica DMi8 equipped with a X-light V2 Confocal Unit spinning disk. The Leica SP8 was equipped with an HC PL APO 40×/1.10 W CORR CS2 objective equipped with Leica LAS-X software (Leica). The Leica DMi8 STP800 (Leica, Bannockburn, IL) equipped with a Lumencor SPECTRA X (Lumencor, Beaverton, OR) with a Hamamatsu ORCA-flash 4.0 V2 CMOS C11440-22CU camera or 89 North–LDI laser with a Photometrics Prime-95B camera taken with a Crest Optics: X-light V2 Confocal Unit spinning disk. Optics used were either HC PL APO 63×/1.40 NA oil CS2, HC PL APO 40×/1.10 NA WCS2 CORR, a 40 × 1.15 N.A. Lamda S LWD, or 100×/1.4 N.A. HC Pl Apo oil emersion objective. Metamorph or VisiView software was used to acquire images. Superresolution 3D-SIM images were acquired on a DeltaVision OMX V4 (GE Healthcare) equipped with a 60×/1.42 NA PlanApo oil immersion lens (Olympus), 405-, 488-, 568-, and 642-nm solid-state lasers and sCMOS cameras. Image stacks of 5–6 µm with 0.125-µm-thick z-sections and 15 images per optical slice (three angles and five phases) were acquired using immersion oil with a refractive index of 1.518. Images were reconstructed using Wiener filter settings of 0.003 and optical transfer functions measured specifically for each channel with SoftWoRx 6.1.3 (GE Healthcare). Images from different color channels were registered using parameters generated from a gold grid registration slide (GE Healthcare) and SoftWoRx 6.1.3 (GE Healthcare).

Image analysis

z-Steps (0.2 µm) of cell volumes are presented as maximum projections using ImageJ. Integrated intensities were measured on sum projections as described in Hoffman *et al.* (2001). Line scans were performed by calculating the normalized fluorescence intensity across a single line; poles were determined as the oldest if they had elevated centrin (as reported in Kuo *et al.*, 2011). Spindle pole integrated intensities were measured from sum confocal projections. Background fluorescence was measured based on values from control shRNA–treated cells and subtracted from both control and cenexin shRNA–treated cells. A ROI was placed over spindle poles (marked with GFP-centrin or cenexin, depending) and the fluorescence intensity was measured. The same ROI was used for all images. Graphs and statistical analysis (unpaired Student's *t* tests or analysis of variance [ANOVA] as labeled) were completed using Graphpad Prism software. Error bars represent ± SEM; $p < 0.05$ were considered to be statistically significant. All images were set to a resolution of 300 DPI or greater after image analysis from raw data.

To quantify PLK1 intensity ratios between poles in zebrafish embryos, a maximum projection was created using a z-stack that encompassed both spindle poles of a metaphase cell. A ROI was drawn around one pole of a single cell within an embryo using FIJI/ImageJ. The same ROI was used for all images. The mean intensity was calculated by subtracting the minimum intensity from that measured region. A ratio was calculated by dividing the value of the pole with the smaller intensity by the value of the pole with the larger intensity. This yielded a value greater or equal to 1. Graphs and statistical analysis (unpaired Student's *t* tests or ANOVA analysis as labeled) were completed using Graphpad Prism software.

ACKNOWLEDGMENTS

This work was supported by National Institutes of Health Grants no. R00GM107355 and no. R01GM127621 (to H.H.) and the Carol Baldwin Foundation of Central New York (to H.H. while at SUNY Upstate Medical University). This work was supported by the U.S. Army Medical Research Acquisition Activity through the FY 16 Prostate Cancer Research Programs under Award no. W81XWH-17-1-0241 (to H.H.). Opinions, interpretations, conclusions, and recommendations are those of the authors and are not necessarily endorsed by the Department of Defense. We thank Patrick Meraldi for providing us the centrin-GFP/CENPA-mCherry HeLa cell line (Gasic *et al.*, 2015) and Patrina Pellet (previously at G.E.) for assistance obtaining SIM images. We thank Dan Bergstralh (University of Rochester), Wenyi Feng, Leszek Kotula, and David Pruyne (SUNY Upstate Medical University) for careful edits and suggestions on earlier versions of this article.

REFERENCES

Burkard ME, Randall CL, Larochelle S, Zhang C, Shokat KM, Fisher RP, Jallepalli PV (2007). Chemical genetics reveals the requirement for Polo-like kinase 1 activity in positioning RhoA and triggering cytokinesis in human cells. Proc Natl Acad Sci USA 104, 4383–4388.

Chen CT, Hehnly H, Yu Q, Farkas D, Zheng G, Redick S, Hung HF, Samtani R, Jurczyk A, Akbarian S, *et al.* (2014). A unique set of centrosome proteins requires pericentrin for spindle-pole localization and spindle orientation. Curr Biol 24, 2327–2334.

Colicino EG, Garrastegui AM, Freshour J, Santra P, Post DE, Kotula L, Hehnly H (2018). Gravin regulates centrosome function through PLK1. Mol Biol Cell 29, 532–541.

Colicino EG, Hehnly H (2018). Regulating a key mitotic regulator, polo-like kinase 1 (PLK1). Cytoskeleton (Hoboken) 75, 481–494.
Conduit PT, Brunk K, Dobbelaere J, Dix CI, Lucas EP, Raff JW (2010). Centrioles regulate centrosome size by controlling the rate of Cnn incorporation into the PCM. Curr Biol 20, 2178–2186.
Conduit PT, Raff JW (2010). Cnn dynamics drive centrosome size asymmetry to ensure daughter centriole retention in *Drosophila* neuroblasts. Curr Biol 20, 2187–2192.
Crasta K, Ganem NJ, Dagher R, Lantermann AB, Ivanova EV, Pan Y, Nezi L, Protopopov A, Chowdhury D, Pellman D (2012). DNA breaks and chromosome pulverization from errors in mitosis. Nature 482, 53–58.
Enver T, Soneji S, Joshi C, Brown J, Iborra F, Omtoft T, Thykjaer T, Maltby E, Smith K, Abu Dawud R, *et al*. (2005). Cellular differentiation hierarchies in normal and culture-adapted human embryonic stem cells. Hum Mol Genet 14, 3129–3140.
Garcia-Martinez J, Bakker B, Schukken KM, Simon JE, Foijer F (2016). Aneuploidy in stem cells. World J Stem Cells 8, 216–222.
Gasic I, Nerurkar P, Meraldi P (2015). Centrosome age regulates kinetochore-microtubule stability and biases chromosome mis-segregation. Elife 4, 1.
Hehnly H, Canton D, Bucko P, Langeberg LK, Ogier L, Gelman I, Santana LF, Wordeman L, Scott JD (2015). A mitotic kinase scaffold depleted in testicular seminomas impacts spindle orientation in germ line stem cells. Elife 4, e09384.
Hehnly H, Chen C-T, Powers CM, Liu H-L, Doxsey S (2012). The centrosome regulates the Rab11-dependent recycling endosome pathway at appendages of the mother centriole. Curr Biol 22, 1944–1950.
Hoffman DB, Pearson CG, Yen TJ, Howell BJ, Salmon ED (2001). Microtubule-dependent changes in assembly of microtubule motor proteins and mitotic spindle checkpoint proteins at PtK1 kinetochores. Mol Biol Cell 12, 1995–2009.
Hung H-F, Hehnly H, Doxsey S (2016). The mother centriole appendage protein cenexin modulates lumen formation through spindle orientation. Curr Biol 26, 793–801.
Ishikawa H, Kubo A, Tsukita S, Tsukita S (2005). Odf2-deficient mother centrioles lack distal/subdistal appendages and the ability to generate primary cilia. Nat Cell Biol 7, 517–524.
Jain AK, Allton K, Iacovino M, Mahen E, Milczarek RJ, Zwaka TP, Kyba M, Barton MC (2012). p53 regulates cell cycle and MicroRNAs to promote differentiation of human embryonic stem cells. PLoS Biol 10, e1001268–16.
Januschke J, Llamazares S, Reina J, Gonzalez C (2011). Drosophila neuroblasts retain the daughter centrosome. Nat Comm 2, 243.
Kimmel CB, Ballard WW, Kimmel SR, Ullmann B, Schilling TF (1995). Stages of embryonic development of the zebrafish. Dev Dyn 203, 253–310.
Kishi K, van Vugt MATM, Okamoto K-I, Hayashi Y, Yaffe MB (2009). Functional dynamics of Polo-like kinase 1 at the centrosome. Mol Cell Biol 29, 3134–3150.
Kobayashi T, Dynlacht BD (2011). Regulating the transition from centriole to basal body. J Cell Biol 193, 435–444.
Kong D, Farmer V, Shukla A, James J, Gruskin R, Kiriyama S, Loncarek J (2014). Centriole maturation requires regulated Plk1 activity during two consecutive cell cycles. J Cell Biol 206, 855–865.
Kuo TC, Chen CT, Baron D, Onder TT, Loewer S, Almeida S, Weismann CM, Xu P, Houghton JM, Gao FB, *et al*. (2011). Midbody accumulation through evasion of autophagy contributes to cellular reprogramming and tumorigenicity. Nat Cell Biol 13, 1214–1223.
Lampson MA, Cheeseman IM (2011). Sensing centromere tension: aurora B and the regulation of kinetochore function. Trends Cell Biol 21, 133–140.
Lee K, Rhee K (2011). PLK1 phosphorylation of pericentrin initiates centrosome maturation at the onset of mitosis. J Cell Biol 195, 1093–1101.
Liu D, Davydenko O, Lampson MA (2012). Polo-like kinase-1 regulates kinetochore-microtubule dynamics and spindle checkpoint silencing. J Cell Biol 198, 491–499.
Maynard S, Swistowska AM, Lee JW, Liu Y, Liu S-T, Da Cruz AB, Rao M, de Souza-Pinto NC, Zeng X, Bohr VA (2008). Human embryonic stem cells have enhanced repair of multiple forms of DNA damage. Stem Cells 26, 2266–2274.
Piel M, Meyer P, Khodjakov A, Rieder CL, Bornens M (2000). The respective contributions of the mother and daughter centrioles to centrosome activity and behavior in vertebrate cells. J Cell Biol 149, 317–330.
Posch M, Khoudoli GA, Swift S, King EM, Deluca JG, Swedlow JR (2010). Sds22 regulates aurora B activity and microtubule-kinetochore interactions at mitosis. J Cell Biol 191, 61–74.
Ramani A, Mariappan A, Gottardo M, Mandad S, Urlaub H, Avidor-Reiss T, Riparbelli M, Callaini G, Debec A, Feederle R, *et al*. (2018). Plk1/Polo phosphorylates Sas-4 at the onset of mitosis for an efficient recruitment of pericentriolar material to centrosomes. Cell Rep 25, 3618–3630.e6.
Schmidt KN, Kuhns S, Neuner A, Hub B, Zentgraf H, Pereira G (2012). Cep164 mediates vesicular docking to the mother centriole during early steps of ciliogenesis. J Cell Biol 199, 1083–1101.
Soung N-K, Kang YH, Kim K, Kamijo K, Yoon H, Seong YS, Kuo YL, Miki T, Kim SR, Kuriyama R, *et al*. (2006). Requirement of hCenexin for proper mitotic functions of polo-like kinase 1 at the centrosomes. Mol Cell Biol 26, 8316–8335.
Soung N-K, Park J-E, Yu L-R, Lee KH, Lee J-M, Bang JK, Veenstra TD, Rhee K, Lee KS (2009). Plk1-dependent and -independent roles of an ODF2 splice variant, hCenexin1, at the centrosome of somatic cells. Dev Cell 16, 539–550.
Vertii A, Bright A, Delaval B, Hehnly H, Doxsey S (2015). New frontiers: discovering cilia-independent functions of cilia proteins. EMBO Rep 16, 1275–1287.
Vertii A, Hung H-F, Hehnly H, Doxsey S (2016). Human basal body basics. Cilia 5, 13.
Vertii A, Kaufman PD, Hehnly H, Doxsey S (2018). New dimensions of asymmetric division in vertebrates. Cytoskeleton (Hoboken) 75, 87–102.
Wang G, Chen Q, Zhang X, Zhang B, Zhuo X, Liu J, Jiang Q, Zhang C (2013). PCM1 recruits Plk1 to the pericentriolar matrix to promote primary cilia disassembly before mitotic entry. J Cell Sci 126, 1355–1365.
Wang X, Tsai J-W, Imai JH, Lian W-N, Vallee RB, Shi S-H (2009). Asymmetric centrosome inheritance maintains neural progenitors in the neocortex. Nature 461, 947–955.
Yamashita YM, Mahowald AP, Perlin JR, Fuller MT (2007). Asymmetric inheritance of mother versus daughter centrosome in stem cell division. Science 315, 518–521.